Zero-Field Splitting Parameter of Mn^{2+} in Zinc Aluminate Single Crystals

M. Bharati[a], V. Singh[a] and R. Kripal[b,*]

[a]*Department of Physics, Nehru Gram Bharti (DU), Jamunipur, Prayagraj, India*
[b]*EPR Laboratory, Department of Physics, University of Allahabad, Prayagraj-211002, India*

Received: 28.12.2023 & Accepted: 14.05.2024

Doi: 10.12693/APhysPolA.146.123 *e-mail: ram_kripal2001@rediffmail.com

A theoretical study of the crystal-field parameters and zero-field splitting parameter of Mn^{2+}-doped zinc aluminate single crystals has been completed with the use of the perturbation theory and the superposition model. The theoretical value of the zero-field splitting parameter D agrees well with the experimental value. This validates the experimental outcome that Mn^{2+} ions substitute at the Zn^{2+} site in zinc aluminate single crystal. Using the parameters of the crystal field and the crystal field analysis program, the optical spectra of Mn^{2+}-doped zinc aluminate crystal are calculated. The calculated and experimental energy values agree with each other reasonably well. Thus, the theoretical approach supports the experiment.

topics: inorganic compounds, single crystal and crystal fields, optical properties, electron paramagnetic resonance

1. Introduction

Electron paramagnetic resonance (EPR) provides information about symmetry at the local site of transition ions doped in different crystals, as well as about the distortions present in the lattice [1–3]. The above studies suggest that the transition ion (d^5) spin Hamiltonian (SH) parameters in crystals are quite sensitive to local distortions. The above parameters may be correlated using microscopic spin Hamiltonian (MSH) theory with optical and structural parameters.

The crystal-field (CF) parameters of the d^5 ion can be obtained using the superposition model (SPM) [4–6]. After that, the CF parameters are used to determine the zero-field splitting (ZFS) parameters [7, 8]. The Mn^{2+} ion of the iron group is interesting due to its $^6S_{5/2}$ ground state [9–11].

SPM was proposed [12] for calculating CF parameters based on the following assumptions:

1. CF at a paramagnetic ion can be expressed as an algebraic sum of the contributions from other ions in the crystal.
2. When the paramagnetic ion is at the origin of a chosen coordinates system, all major CF contributions from every ion in the crystal are axially symmetric with respect to its position vector.
3. Only neighboring or coordinated ions should be considered for their CF contributions.
4. The CF contributions from a single ion (ligand) are transferable across different host crystals.

The first assumption implies the validity of the superposition principle in the description of CF, while the axial symmetry assumption (2) allows us to freely transform one coordinate system to another. However, a more restrictive form of assumption (3) is often adopted, in which only the nearest neighbor ions are considered. The last assumption (4) on ligand transferability means that the CF contributions from a single ligand depend only on the ligand type and its distance from the paramagnetic ion. In order to perform an SPM analysis of the CF splitting, an almost pre-requisite condition is to have a reliable set of polar coordinates (R_L, θ_L, Φ_L) for all the ligands in question, as obtained from X-ray data of the host crystal. If transition metal ions are doped as impurities, they will probably produce a certain amount of local distortion or lattice relaxation due to a mismatch in ionic charge, ionic size, and/or inter-ionic bonding. If there is a sufficient number of CF parameters, a linear or nonlinear least-square fit can be applied to these CF parameters to find the fitted values of the SPM intrinsic parameters and the power-law exponents. A critical analysis of the experimental spin Hamiltonian parameters for Mn^{2+} and Fe^{3+} in CaO and MgO crystals has been made [13], verifying that CF for $3d$ ions satisfies the superposition principle and provides explicit values of the SPM parameters for the EPR data. A rigorous lattice relaxation

model was developed [14] to calculate locally distorted ligand positions for Eu^{2+} at the orthorhombic sites in various alkali halides. A similar approach was applied [15] to a reliable set of ligand distances calculated for alkaline earth oxides to find sets of the SPM intrinsic parameters ($R_0 = 2.0$ Å) for Mn^{2+}- and Fe^{3+}-doped MgO, CaO, and SrO. The result was: $\bar{b}_2 = (-1552 \pm 48) \times 10^{-4}$ cm^{-1} (for Fe^{3+}) and $\bar{b}_2 = (-6440 \pm 113) \times 10^{-4}$ cm^{-1} (for Mn^{2+}) with fixed $t_2 = 16$ for both ions; $\bar{b}_4 = (9.9 \pm 0.8) \times 10^{-4}$ cm^{-1} (for Fe^{3+} and Mn^{2+}) with fixed $t_4 = (16 \pm 4)$ for both ions. For the separate fit of t_2, the fitted values were 17.7 and 14.4 for Mn^{2+} and Fe^{3+}, respectively.

Zinc aluminate, or $ZnAl_2O_4$, is a spinel-structured semiconductor having a band gap of $E_g = 3.8$ eV. It has been thoroughly investigated as a luminophore host substance for various applications, e.g., in mechano–optical stress sensors, thin-film electroluminescence displays, and stress imaging apparatuses [16–19]. $ZnAl_2O_4$ spinel possesses special properties such as improved diffusion, ductility, and high thermal stability. Because of these special properties, it is used as an optical coating material and at high temperatures. In addition, $ZnAl_2O_4$ is also employed in a variety of catalytic processes, including dehydration, cracking, hydrogenation, and dehydrogenation [20–23]. The studies are carried out on $ZnAl_2O_4$ phosphors doped with transition ions and rare earth ions [24–28], where there is a broad range of potential industrial uses. Mn^{2+} luminescence produces a cheap red- or green-emitting phosphor. Mn-doped $ZnAl_2O_4$ thin films prepared by spray pyrolysis exhibit vivid green cathodoluminescence at low excitation voltage [26].

EPR measurements on Mn^{2+}-doped zinc aluminate ($ZnAl_2O_4$) single crystals at 300 K have been reported [29]. The current investigation determines the CF parameters using SPM, and these parameters with MSH theory give the ZFS parameter for the Mn^{2+} ions at the axial center in the $ZnAl_2O_4$ single crystal at 300 K. The experimental value and the ZFS parameter D, as determined by SPM, agree well [20].

2. Crystal structure

With "A" denoting a metal cation occupying a tetrahedral site and "B" denoting Al occupying octahedral sites of a cubic crystal, $ZnAl_2O_4$ has the general formula AB_2O_4. The cubic unit cell that makes up the crystal spinel structure (AB_2O_4) is an element of the space group $Fd3m$. AB_2O_4 patterns are found in eight per unit cell. Only eight tetrahedral sites (on Wyckoff positions 8a $(1/8, 1/8, 1/8)$ and sixteen octahedral sites (on Wyckoff positions 16d $(1/2, 1/2, 1/2)$) in the direct spinel structure are occupied by the A and B cations, respectively, while the oxygen anions completely occupy the 32e

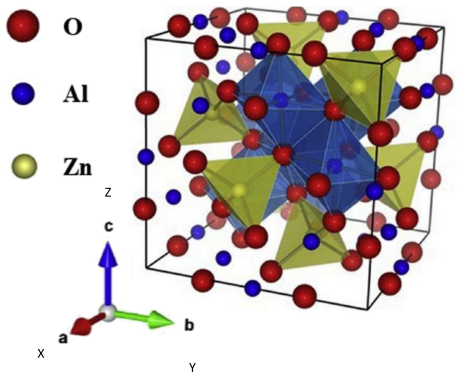

Fig. 1. Crystal structure of $ZnAl_2O_4$ together with axes (SAAS — symmetry adopted axes system).

positions [29, 30]. Zn^{2+} cations are found in the 8a sites of $ZnAl_2O_4$, also known as gahnite, while Al^{3+} cations may occupy part of the 16d sites. The lattice constant is $a = 8.0891$ Å [29]. The oxygen coordination around Zn^{2+} is shown in Fig. 1 (courtesy of Menon et al. [31]). The site symmetry around Mn^{2+} ions may be taken to be axial (the point symmetry group is D_{2d} [32]), as indicated by the EPR study of Mn^{2+}-doped $ZnAl_2O_4$ [30].

The laboratory axes (x, y, z) are selected so that they align with the crystallographic axes (a, b, c). The symmetry adopted axes are labeled (X, Y, Z). The principal Z axis of g and D tensors of Mn^{2+} ions is found to correspond to the crystallographic c axis. The two other axes (X, Y) are perpendicular to the Z axis (Fig. 1). This suggests that in the $ZnAl_2O_4$ crystal, Mn^{2+} takes the place of Zn^{2+} with approximately axial symmetry. Mn^{2+} ion's ionic radius (0.066 nm, tetrahedral coordination) is marginally larger than Zn^{2+} ionic radius (0.060 nm), indicating that Mn^{2+} ion can sit at the position of Zn^{2+} with certain distortion.

3. Theoretical investigation

The SH of $3d^5$ ion in the axially symmetric crystal field is given as [33–35]

$$\begin{aligned}
\mathcal{H} &= \mathcal{H}_{\mathrm{Ze}} + \mathcal{H}_{\mathrm{ZFS}} + \mathcal{H}_{\mathrm{hfs}} = \\
&\mu_{\mathrm{B}} \boldsymbol{B} \cdot g \boldsymbol{S} + \sum_{k,q} B_k^q O_k^q \left(S_x, S_y, S_z\right) + A(\boldsymbol{I} \cdot \boldsymbol{S}) = \\
&\mu_{\mathrm{B}} \boldsymbol{B} \cdot g \boldsymbol{S} + D \left\{ S_z^2 - S\left(S+1\right) \right\} \\
&+ \frac{a}{6} \left[S_x^4 + S_y^4 + S_z^4 - \frac{1}{5} S\left(S+1\right) \left(3S^2 + 3S - 1\right) \right] \\
&+ \frac{F}{180} \Big\{ 35 S_z^4 - 30 S\left(S+1\right) S_z^2 + 25 S_z^2 \\
&- 6S\left(S+1\right) + 3S^2 \left(S+1\right)^2 \Big\} + A\left(\boldsymbol{I} \cdot \boldsymbol{S}\right), \qquad (1)
\end{aligned}$$

TABLE I

Atomic coordinates in $ZnAl_2O_4$ crystal and spherical polar coordinates of ligands (R, θ, Φ).

	Position of Mn^{2+} (fractional)	Ligands [Å]			Spherical co-ordinates of ligands		
		x	y	z	R [nm]	θ [degree]	Φ [degree]
Site: Substitutional Zn (0.125, 0.125, 0.125)	O1	0.2640	0.2640	0.2640	0.1947	54.73	45.00
	O2	0.2640	−0.0140	−0.0140	0.1947	125.26	−45.00
	O3	−0.2640	−0.2640	−0.2640	0.5450	125.26	45.00
	O4	−0.2640	1.0140	1.0140	1.0645	47.50	−66.37

where B_k^q are the ZFS parameters associated with the extended Stevens operators O_k^q [8], which depend on the spin operators $\boldsymbol{S} = (S_x, S_y, S_z)$. The very first term describes electronic Zeeman interaction, where the external magnetic field is $\boldsymbol{B}$, the Bohr magneton is represented by μ_{B}, and g is the spectroscopic splitting factor. The second-rank axial, fourth-rank cubic, and fourth-rank axial ZFS terms are the second, third, and fourth terms, respectively, in the third, fourth, and fifth lines of (1) [10]. The hyperfine interaction term is the fifth term. The effective spin vector, second-order axial, fourth-rank cubic, and fourth-rank axial ZFS parameters are denoted by the letters S, D, a, and F, respectively. The Zeeman electronic interaction is taken to be isotropic for Mn^{2+} ions [10, 12, 36].

For a d^5 ion, the Hamiltonian is provided as

$$\mathcal{H} = \mathcal{H}_0 + \mathcal{H}_{cf} + \mathcal{H}_{so}, \tag{2}$$

where

$$\mathcal{H}_{cf} = \sum\nolimits_{kq} B_{kq} C_q^k \tag{3}$$

is the Hamiltonian of the crystal field, while $\mathcal{H}_{so}$ and $\mathcal{H}_0$ are spin–orbit (SO) coupling and the free ion Hamiltonian, respectively. Since the spin–spin coupling is very small [37–39], its contribution is neglected in (2). The perturbation term is the crystal field of the SO interaction [40–42]. For $3d^5$ ions in axial symmetry, the SO contribution to the ZFS parameter D is provided as [41]

$$D^{(4)}(\mathrm{SO}) = \frac{\xi^2}{P^2}\left[\frac{14B_{44}^2 - 5B_{40}^2}{63G} - \frac{3B_{20}\,(B_{20} - 14\xi)}{70D}\right], \tag{4}$$

where $P = 7(B + C)$, $G = 10B + 5C$, and $D = 17B + 5C$. Here, P, G, and D provide the energy differences between the ground sextet and the excited quartets. The electron–electron repulsion is represented by the Racah parameters B and C. In (4), only the fourth-order term is included because other perturbation terms are insignificant [41, 42]. The relations $B = N^4 B_0$, $C = N^4 C_0$, and $\xi = N^2 \xi_0$ represent the parameters B, C, and ξ in terms of the average covalency parameter N, where B_0, C_0, and ξ_0 are the Racah parameters and the spin-orbit coupling parameter for free ion, respectively [43]. For Mn^{2+} ion, we take here $B_0 = 960$ cm^{-1}, $C_0 = 3325$ cm^{-1}, $\xi_0 = 336$ cm^{-1} [10]. Using equation

$$N = \frac{1}{2}\left(\sqrt{B/B_0} + \sqrt{C/C_0}\right), \tag{5}$$

N can be obtained by taking the values of Racah parameters ($B = 760$ cm^{-1}, $C = 2714$ cm^{-1}) from optical absorption of Mn^{2+} ion in $ZnAl_2O_4$ crystal having oxygen ligands in tetrahedral coordination [31].

The ZFS parameter D is obtained from (4) after determining the CF parameters for Mn^{2+} in $ZnAl_2O_4$ single crystal using SPM. A comparable technique has been employed to find the ZFS parameters in many other works [44].

In order to interpret the crystal-field splitting in various crystals, SPM is effectively used. Also, the aforementioned model has been applied for $3d^n$ ions [41]. Using this model, the parameters B_{kq} of the crystal field are determined from the equations [45, 46]

$$B_{20} = -2\overline{A}_2\left(\frac{R_0}{R_{10}+\Delta R_1}\right)^{t_2} - 4\overline{A}_2\left(\frac{R_0}{R_{20}+\Delta R_2}\right)^{t_2}, \tag{6}$$

$$B_{40} = 16\overline{A}_4\left(\frac{R_0}{R_{10}+\Delta R_1}\right)^{t_4} + 12\overline{A}_4\left(\frac{R_0}{R_{20}+\Delta R_2}\right)^{t_4}, \tag{7}$$

$$B_{44} = 2\sqrt{70}\,\overline{A}_4\left(\frac{R_0}{R_{20}+\Delta R_2}\right)^{t_4}, \tag{8}$$

where R_0 is the reference distance, which is typically calculated as the axially symmetric mean of the four bond lengths; ΔR_1 and ΔR_2 give the distortion parameters; $\overline{A}_2$, $\overline{A}_4$, and t_k denote the intrinsic parameters and the power law exponent, respectively.

4. Results and discussion

The position of Mn^{2+} ion and spherical polar coordinates of ligands are shown in Table I. Two of the four Mn^{2+}–O^{2-} bond lengths have an average value of $R_{10} = 0.6296$ nm, and the remaining two have an average value of $R_{20} = 0.3698$ nm. In tetrahedral coordination, $\overline{A}_4(R_0) = (-\frac{27}{16})Dq$ [5]. The ratio $\frac{\overline{A}_2}{\overline{A}_4}$ for $3d^5$ ions is between 8 and 12 [41, 42]. For the Mn^{2+} ion, the power law exponents are determined to be equal to $t_2 = 3$ and

TABLE II

Crystal-field parameters and zero-field splitting parameters of Mn^{2+}-doped $ZnAl_2O_4$ single crystal.

ΔR_1 [nm]	ΔR_2 [nm]	R_0 [nm]	Crystal-field parameters [cm^{-1}]			Zero-field splitting parameter D ($\times 10^{-4}$) [cm^{-1}]
			B_{20}	B_{40}	B_{44}	
−0.11174	−0.11178	0.211	14802.64	−1886.85	−2604.57	301.0
0.00000	0.00000	0.211	5216.476	−155.31	−209.816	12.3
						Exp. 301.0

TABLE III

Observed and calculated (CFA package) energy band positions [cm^{-1}] of Mn^{2+}-doped $ZnAl_2O_4$ single crystal.

Transition from $^6A_{1g}(S)$ to	Observed [31]	Calculated
$^4T_{1g}(G)$	20000	19135, 19225, 19492, 19571, 20624, 20784
$^4T_{2g}(G)$	22124	21468, 21492, 22674, 22679, 22684, 22685
$^4E_g(G)/^4A_{1g}(G)$	23474	22698, 22739, 22802, 22888
$^4T_{2g}(D)$	25840	25129, 25136, 25459, 25490,25539,25596
$^4T_{1g}(P)$		30148, 30420, 30554,30752, 31146, 31156
$^4A_{2g}(F)$	35971	35789, 35955
$^4T_{1g}(F)$		36213, 36496, 36678,36829, 37060, 37392
$^4T_{2g}(F)$		38085, 38345, 38466, 38573, 38576, 38663

Input parameters: number of free ion parameters = 5; number of d shell electrons = 5; number of fold for rotational site symmetry = 1; Racah parameters in A, B, C, spin–orbit coupling constant, and Trees correction are 0, 760, 2714, 336, and 76 cm^{-1}, respectively; numbers of crystal-field parameters = 3; B_{20}, B_{40}, B_{44} are taken from Table II; spin–spin interaction parameter $M_0 = 0.2917$; spin–spin interaction parameter $M_2 = 0.0229$; spin–other-orbit interaction parameter $M_{00} = 0.2917$; spin–other-orbit interaction parameter $M_{22} = 0.0229$; magnetic field $\boldsymbol{B} = 0.0$ Gauss; angle between magnetic field $\boldsymbol{B}$ and Z-axis = 0.00 degree.

$t_4 = 7$. To obtain the intrinsic parameter values in SPM, semi-*ab initio* calculations are performed for other transition ions; the same method is adopted there.

The values of B, C, and Dq are derived from the optical absorption study [31] and are 760, 2714, and 378 cm^{-1}, respectively. First, no local distortion is included when D's value is computed. This can be accomplished by taking $\frac{\overline{A_2}}{A_4} = 10$ and $R_0 = 0.211$ nm, which is marginally larger than the total ionic radii of $Mn^{2+} = 0.066$ nm and of $O^{2-} = 0.138$ nm (four coordination). The following B_{kq} parameters are used: $B_{20} = 5216.476$ cm^{-1}, $B_{40} = -155.31$ cm^{-1}, $B_{44} = -209.816$ cm^{-1}. As a result, the D value is $|D| = 12.3 \times 10^{-4}$ cm^{-1}. EPR study gives D the experimental value of D as $|D| = 301.0 \times 10^{-4}$ cm^{-1} [29]. From the above, it is evident that the experimental value is greater than the theoretical value.

Now, we take the local distortions as $\Delta R_1 = -0.11174$ nm and $\Delta R_2 = -0.11178$ nm, $R_0 = 0.211$ nm and ratio $\frac{\overline{A_2}}{A_4} = 10$. Table II shows the calculated B_{kq} parameters and D being equal to $|D| = 301.0 \times 10^{-4}$ cm^{-1}, which is in excellent agreement with the experimental result, i.e., $|D| = 301.0 \times 10^{-4}$ cm^{-1}. Taking B_{kq} parameters and the CFA program [47, 48], the optical spectra of Mn^{2+}-doped $ZnAl_2O_4$ single crystal are calculated. The energy levels of Mn^{2+} ion are computed by diagonalizing the complete Hamiltonian within the $3d^N$ basis of states in the intermediate crystal-field coupling scheme. Table III provides the calculated energy values (input parameters are given below the table) along with the experimental values [31] for comparison. It is found from Table III that there is a reasonable agreement between the computed and experimental results. The energy values obtained without considering the distortion were quite different from the experimental values and are therefore not given here. Thus, the theoretical study confirms the results of the experimental investigation.

5. Conclusions

In $ZnAl_2O_4$ single crystal, the zero-field splitting parameter D for Mn^{2+} was calculated using the superposition model and perturbation theory. The theoretical D value fits nicely with the experimental value when distortion is included in the calculation. The theoretical investigation shows that the Mn^{2+} ion occupies the Zn^{2+} site, which supports the results of the experimental

EPR study. It is found from the CF energy calculation that there is a reasonable agreement between the computed and experimental energy values. Thus, the theoretical study confirms the experimental results. The procedure applied here may be used in several other ion-host systems to explore scientific and industrial applications of different crystals.

Acknowledgments

The authors are grateful to the Head of the Department of Physics for providing the departmental facilities and to Professor C. Rudowicz, Faculty of Chemistry, A. Mickiewicz University, Poznań, Poland, for the CFA program.

References

[1] P. Gnutek, Z. Y. Yang, C. Rudowicz, *J. Phys. Condens. Matter* **21**, 455402 (2009).

[2] Z.Y. Yang, Y. Hao, C. Rudowicz, Y.Y. Yeung, *J. Phys. Condens. Matter* **16**, 3481 (2004).

[3] C. Rudowicz, S.K. Misra, *Appl. Spectrosc. Rev.* **36**, 11 (2001).

[4] S.K. Misra in: *Handbook of ESR*, Vol. 2, Eds. C.P. Poole Jr., H.A. Farach, Springer, New York 1999, Ch. IX, p. 291.

[5] H. Anandlakshmi, K. Velavan, I. Sougandi, R. Venkatesan, P.S. Rao, *Pramana* **62**, 77 (2004).

[6] C. Rudowicz, P. Gnutek, M. Acikgoz, *Appl. Spectr. Rev.* **54**, 673 (2019).

[7] S. Pandey, R. Kripal, A. K. Yadav, M. Açıkgöz, P. Gnutek, C. Rudowicz, *J. Lumin.* **230**, 117548 (2020).

[8] C. Rudowicz, M. Karbowiak, *Coord. Chem. Rev.* **287**, 28 (2015).

[9] I. Stefaniuk, *Opto-Electronics Rev.* **26**, 81 (2018).

[10] A. Abragam, B. Bleaney, *Electron Paramagnetic Resonance of Transition Ions*, Clarendon Press, Oxford 1970.

[11] D.J. Newman, B. Ng, *Crystal Field Handbook*, Cambridge University Press, Cambridge 2000.

[12] D.J. Newman, B. Ng, *Rep. Prog. Phys.* **52**, 699 (1989).

[13] D.J. Newman, E. Siegel, *J. Phys. C Solid State Phys.* **9**, 4285 (1976).

[14] Y.Y. Yeung, D.J. Newman, *J. Phys. C Solid State Phys.* **21**, 537 (1988).

[15] Y.Y. Yeung, *J. Phys. C Solid State Phys.* **21**, 2453 (1988).

[16] S.K. Sampath, J.F. Cordaro, *J. Am. Ceram. Soc.* **81**, 649 (1998).

[17] R. Roesky, J. Weiguny, H. Bestgen, U. Dingerdissen, *Appl. Catal. A General* **176**, 213 (1999).

[18] S.K. Sampath, D.G. Kandive, R. Pandey, *J. Phys. Condens. Matter* **11**, 3635 (1999).

[19] H. Matsui, C.N. Xu, H. Tateyama, *Appl. Phys. Lett.* **78**, 1068 (2001).

[20] M.C. Marion, E. Garbowski, M. Primet, *J. Chem. Soc. Faraday Trans.* **11**, 1795 (1991).

[21] F. Le Peltier, P. Chaumette, J. Saussey, M.M. Bettahar, J.C. Lavalley, *J. Mol. Catal. A* **122**, 131 (1997).

[22] M. A. Valenzuela, G. Aguilar, P. Bosch, H. Armendariz, P. Salas, A. Montoya, *Catal. Lett.* **15**, 179 (1992).

[23] J. Wrzyszcz, M. Zawadzki, J. Trawczynski, H. Grabowska, W. Mista, *Appl. Catal. A General* **210**, 263 (2001).

[24] D. Jia, X.-J. Wang, E. van der Kolk, W.M. Yen, *Opt. Commun.* **204**, 247 (2002).

[25] M. García-Hipólito, J. Guzmán-Mendoza, E. Martínez, O. Alvarez-Fregoso, C. Falcony, *Phys. Status Solidi (a)* **201**, 1510 (2004).

[26] Z. Lou, J. Hao, *Appl. Phys. A* **80**, 151 (2005).

[27] S.F. Wang, F. Gu, M.K. Lü, X.F. Cheng, W.G. Zou, G.J. Zhou, S.M. Wang, Y.Y. Zhou, *J. Alloys Compd.* **394**, 255 (2005).

[28] B. Cheng, S. Qu, H. Zhou, Z. Wang, *Nanotechnology* **17**, 2982 (2006).

[29] V. Singh, R.P.S. Chakradhar, J.L. Rao, D.K. Kim, *J. Lumin.* **128**, 394 (2008).

[30] J. Popovic, B. Grzeta, B. Rakvin, E. Tkalcec, M. Vrankic, S. Kurajica, *J. Alloys Compds.* **509**, 8487 (2011).

[31] S.G. Menon, A.K. Kunti, S.D. Kulkarni, R. Kumar, M. Jain, D. Poelman, J.J. Joos, H.C. Swart, *J. Lumin.* **226**, 117482 (2020).

[32] C. Rudowicz, M. Açıkgöz, M. Karbowiak, *Coord. Chem. Rev.* **512**, 215865 (2024).

[33] M.G. Zhao, M.L. Du, G.Y. Sen, *J. Phys. C Solid State Phys.* **18**, 3241 (1985).

[34] W.L. Yu, *Phys. Rev. B* **39**, 622 (1989).

[35] Z.Y. Yang, *J. Phys. Condens. Matter* **12**, 4091 (2000).

[36] W.L. Yu, M.G. Zhao, *Phys. Rev. B* **37**, 9254 (1988).

[37] Z.Y. Yang, C. Rudowicz, Y.Y. Yeung, *Physica B* **348**, 151 (2004).

[38] C. Rudowicz, H.W.F. Sung, *Physica B* **300**, 1 (2001).

[39] C.J. Radnell, J.R. Pilbrow, S. Subramanian, M.T. Rogers, *J. Chem. Phys.* **62**, 4948 (1975).

[40] J.A. Weil, J.R. Bolton, *Electron Paramagnetic Resonance: Elementary Theory and Practical Applications*, 2nd ed., Wiley, New York 2007.

[41] W.L. Yu, M.G. Zhao, *J. Phys. C Solid State Phys.* **17**, L525 (1984).

[42] J.F. Clare, S.D. Devine, *J. Phys. C Solid State Phys.* **17**, L581 (1984).

[43] T.H. Yeom, S.H. Choh, M.L. Du, M.S. Jang, *Phys. Rev. B* **53**, 3415 (1996).

[44] W.L. Yu, M.G. Zhao, *Phys. Stat. B* **140**, 203 (1987).

[45] Y.Y. Yeung, in: *Optical Properties of 3d-Ions in Crystals, Spectroscopy and Crystal Field Analysis*, Eds. M.G. Brik, N.M. Avram, Springer Heidelberg, New York 2013, Ch. 3, p. 95.

[46] Q. Wei, *Acta Phys. Pol. A* **118**, 670 (2010).

[47] Y.Y. Yeung, C. Rudowicz, *J. Comput. Phys.* **109**, 150 (1993).

[48] Y.Y. Yeung, C. Rudowicz, *Comput. Chem.* **16**, 207 (1992).